Int. J. Solids Structures, 1977, Vol. 13, pp. 1157–1171. Pergamon Press. Printed in Great Britain

ELASTODYNAMIC RESPONSE OF A WEDGE TO SURFACE PRESSURES

J. D. Achenbach and R. P. Khetan

Department of Civil Engineering, Northwestern University, Evanston, IL 60201, U.S.A.

(Received 1 February 1977; revised 9 May 1977)

Abstract—An elastic wedge of interior angle $\kappa\pi$, where $1 < \kappa \leq 2$, is subjected to the impact of spatially uniform pressures on its faces. The application of the pressures produces a system of longitudinal waves, transverse waves and head waves. In this paper the elastodynamic stress singularity in the circumferential stress at the vertex of the wedge is analyzed. The analysis is based on self-similarity of first-order time derivatives of the displacement potentials. By means of appropriate transformations the statement of the problem is reduced to two Laplace's equations, whose solutions in half-planes are coupled along the real axes. The solutions to this system are obtained by using elements of analytic function theory, together with summations over Chebychev polynomials along the real axes.

1. INTRODUCTION

The elastic wedge of vertex angle $\kappa\pi$, where $\kappa \neq 1$, which is subjected to stress boundary conditions on its faces, so far has resisted all attempts to obtain analytical elastodynamic solutions. An excellent review article, which discusses various mathematical techniques that have been tried with limited success, was written by Knopoff[1]. The kind of elastodynamic problems that have been solved successfully for the wedge geometry, are for mixed boundary conditions on the faces, i.e. when one displacement component and one stress component are prescribed, see e.g. Refs. [2–4]. The difficulty is, that an integral transform which can accommodate stress boundary conditions, does not exist.

For the quarter plane there have been numerical approaches by finite difference methods, see e.g. [5]. It is presumably also possible to obtain numerical results by the finite element method, but it remains obviously desirable to have a method of solution which is essentially analytical, and which, if necessary, uses numerical work only in the very last stages.

In this paper we take advantage of the self-similarity of certain field variables for certain boundary conditions, to reduce the problem of the transient response of a wedge to the solution in half-plane regions of a set of two Laplace's equations which govern the first-order time derivatives of the displacement potentials. The solutions to these Laplace's equations are coupled along the real axes of the half-planes, by conditions which stem from the conditions along the faces of the wedge and along the wavefronts. The solutions are obtained by using complex function theory in conjuction with summations over Chebyshev polynomials. Special attention is devoted to the computation of an elastodynamic stress intensity factor for the circumferential stress at the vertex.

2. FORMULATION OF THE PROBLEM

A spatially uniform pressure is applied to the faces of a solid wedge of vertex angle $\kappa\pi$, while the faces remain free of shear stresses. The surface pressure generates a state of elastodynamic plane strain, which is described by displacement components $u_r(r, \theta, t)$ and $u_\theta(r, \theta, t)$, and stress components $\tau_r(r, \theta, t)$, $\tau_\theta(r, \theta, t)$ and $\tau_{\theta r}(r, \theta, t)$. The system of polar coordinates is fixed at the vertex of the wedge, such that $\theta = 0$ is the bisector of the vertex angle. The geometry is shown in Fig. 1. In this paper we let $1 < \kappa \leq 2$. The cases $\kappa = 1$ and $\kappa = 2$ correspond to a half-plane and a plane with a semi-infinite slit, respectively.

The material of the wedge is homogeneous, isotropic and linearly elastic. A complete statement of the equations governing elastodynamic problems is given in [6]. Here it should suffice to state that in the usual manner the displacement components are expressed in terms of displacement potentials as

$$u_r = \frac{\partial \varphi}{\partial r} + \frac{1}{r}\frac{\partial \psi}{\partial \theta}, \quad u_\theta = \frac{1}{r}\frac{\partial \varphi}{\partial \theta} - \frac{\partial \psi}{\partial r} \tag{2.1a,b}$$

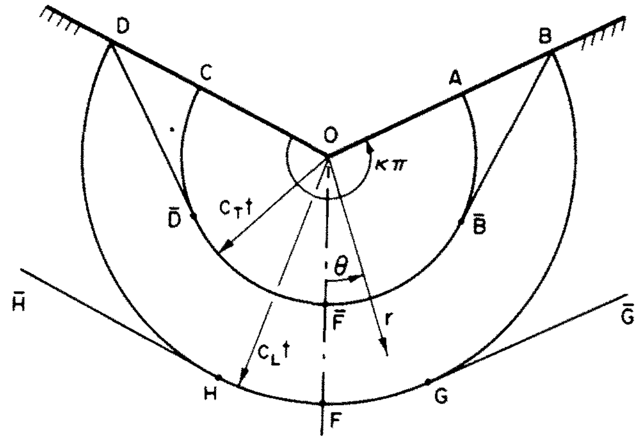

Fig. 1. Pattern of wavefronts in an elastic wedge, due to impulsive uniform pressure on the faces.

where $\varphi(r, \theta, t)$ and $\psi(r, \theta, t)$ satisfy uncoupled wave equations

$$\nabla^2\varphi = \frac{1}{c_L^2}\ddot{\varphi}, \quad c_L^2 = \frac{\lambda + 2\mu}{\rho} \tag{2.2}$$

$$\nabla^2\psi = \frac{1}{c_T^2}\ddot{\psi}, \quad c_T^2 = \frac{\mu}{\rho} \tag{2.3}$$

$$\nabla^2 = \frac{\partial^2}{\partial r^2} + \frac{1}{r}\frac{\partial}{\partial r} + \frac{1}{r^2}\frac{\partial^2}{\partial \theta^2}. \tag{2.4}$$

The boundary conditions are taken as

$$\theta = \pm\frac{1}{2}\kappa\pi, \quad \tau_\theta = -\tau_0\delta(t) \tag{2.5}$$

$$\tau_{\theta r} = 0 \tag{2.6}$$

where $\delta(t)$ is the Dirac delta function, which is selected for convenience. The response to pressure of more general time variation can be obtained later by superposition considerations. The wedge is initially at rest, i.e.

$$t < 0 \quad u_r(r, \theta, t) = \dot{u}_r(r, \theta, t) \equiv 0 \tag{2.7}$$

$$u_\theta(r, \theta, t) = \dot{u}_\theta(r, \theta, t) \equiv 0. \tag{2.8}$$

The pattern of wavefronts is shown in Fig. 1. The surface pressures generate plane longitudinal waves with wavefronts $G\bar{G}$ and $H\bar{H}$, while the vertex gives rise to cylindrical longitudinal and transverse waves, DHFGB and $C\bar{D}\bar{F}\bar{B}A$, respectively. In addition, there are headwaves in the triangular regions $CD\bar{D}$ and $AB\bar{B}$.

3. SELF-SIMILAR SOLUTIONS

For a wedge subjected to surface stresses given by eqns (2.5) and (2.6), there is no characteristic length in the geometry, nor is there a characteristic length in the boundary conditions. It can then be expected that certain derivatives of the field variables are self-similar. This means that they depend on r/t and θ, rather than on r, θ and t, separately. Self-similar solutions in elastodynamics were discussed in [7–10] and [6, p. 154]. The transient response of a wedge in antiplane strain was analyzed on the basis of self-similarity in [11]. For the boundary conditions given by eqn (2.5) the displacement components u_r and u_θ, and the time-derivatives of the potentials $\dot{\varphi}$ and $\dot{\psi}$ are self-similar.

The appropriate self-similar solutions are obtained by introducing the new variable

$$s = r/t. \tag{3.1}$$

The equations governing $\dot{\varphi}(s, \theta)$ and $\dot{\psi}(s, \theta)$ then follow from eqns (2.2) and (2.3) as

$$s^2 \frac{\partial^2 \dot{\varphi}}{\partial s^2} + s \frac{\partial \dot{\varphi}}{\partial s} + \frac{\partial^2 \dot{\varphi}}{\partial \theta^2} = \frac{s^2}{c_L^2} \frac{\partial}{\partial s} \left(s^2 \frac{\partial \dot{\varphi}}{\partial s} \right) \tag{3.2}$$

$$s^2 \frac{\partial^2 \dot{\psi}}{\partial s^2} + s \frac{\partial \dot{\psi}}{\partial s} + \frac{\partial^2 \dot{\psi}}{\partial \theta^2} = \frac{s^2}{c_T^2} \frac{\partial}{\partial s} \left(s^2 \frac{\partial \dot{\psi}}{\partial s} \right). \tag{3.3}$$

In terms of s and θ the particle velocities are

$$r\dot{u}_r = -s^2 \frac{\partial u_r}{\partial s} = s \frac{\partial \dot{\varphi}}{\partial s} + \frac{\partial \dot{\psi}}{\partial \theta} \tag{3.4}$$

$$r\dot{u}_\theta = -s^2 \frac{\partial u_\theta}{\partial s} = \frac{\partial \dot{\varphi}}{\partial \theta} - s \frac{\partial \dot{\psi}}{\partial s}. \tag{3.5}$$

Similarly, by substituting the displacement potentials in Hooke's law, and taking derivatives with respect to time, we find after introducing $s = r/t$, and integrating with respect to s:

$$\frac{rc_T}{\mu} \tau_\theta = -\left[1 - 2 \left(\frac{c_T}{s} \right)^2 \right] \frac{s^2}{c_T} \frac{\partial \dot{\varphi}}{\partial s} + 2 \frac{c_T}{s} \frac{\partial \dot{\psi}}{\partial \theta} \tag{3.6}$$

$$\frac{rc_T}{\mu} \tau_{r\theta} = -2 \frac{c_T}{s} \frac{\partial \dot{\varphi}}{\partial \theta} - \left[1 - 2 \left(\frac{c_T}{s} \right)^2 \right] \frac{s^2}{c_T} \frac{\partial \dot{\psi}}{\partial s}. \tag{3.7}$$

Let us now return to the governing equations for $\dot{\varphi}$ and $\dot{\psi}$, and note that (3.2) and (3.3) are elliptic for $s \leq c_L$ and $s \leq c_T$, respectively. By using the Chaplygin transformation

$$\cosh \beta_L = c_L/s. \tag{3.8}$$

Equation (3.2) reduces to Laplace's equation

$$\frac{\partial^2 \dot{\varphi}}{\partial \beta_L^2} + \frac{\partial^2 \dot{\varphi}}{\partial \theta^2} = 0. \tag{3.9}$$

Similarly, the transformation

$$\cosh \beta_T = c_T/s \tag{3.10}$$

reduces eqn (3.3) to

$$\frac{\partial^2 \dot{\psi}}{\partial \beta_T^2} + \frac{\partial^2 \dot{\psi}}{\partial \theta^2} = 0. \tag{3.11}$$

For $s > c_T$, the transformation

$$\cos \alpha_T = c_T/s \tag{3.12}$$

reduces eqn (3.3) to the wave equation

$$\frac{\partial^2 \dot{\psi}}{\partial \alpha_T^2} - \frac{\partial^2 \dot{\psi}}{\partial \theta^2} = 0. \tag{3.13}$$

The transformations (3.8) and (3.10) map the cylindrical regions in the physical plane $(-(1/2)\kappa\pi \leq \theta \leq (1/2)\kappa\pi,\ s < c_L$ and $s < c_T)$ into strips in the $\theta_L - \beta_L$ and $\theta_T - \beta_T$ planes, respectively. The subscripts in θ_L and θ_T are introduced simply for convenience of notation. The strips are shown in Fig. 2, where the positions of the various points are also indicated. In these strips, $\dot{\varphi}$ and $\dot{\psi}$ are solutions of Laplace's eqns (3.9) and (3.11), respectively. The boundary conditions on the strips follow from the conditions in the physical plane, on the faces of the wedge, and along the wavefronts.

Some of the conditions in the physical plane are simple, and they are immediately transferable to the corresponding line segments in the strips. Thus, we have $\dot{\varphi} = 0$ along GFH, while $\dot{\psi} = 0$ along $\bar{B}\bar{F}\bar{D}$. Along BG and DH, we have $\dot{\varphi} = -\tau_0/\rho$, which is the value corresponding to the plane waves. For $t > 0$ we have $\tau_\theta = 0$ and $\tau_{\theta r} = 0$ along OA and OC, which gives rise to conditions coupling $\partial\dot{\varphi}/\partial\beta_L$ and $\partial\dot{\psi}/\partial\theta_T$, and $\partial\dot{\psi}/\partial\beta_T$ and $\partial\dot{\varphi}/\partial\theta_L$, if the transformations (3.8) and (3.10) are introduced into eqns (3.6) and (3.7). The conditions along AB, A$\bar{B}$, CD and C$\bar{D}$ require some more extensive consideration.

In the headwave regions, $\dot{\psi}$ is governed by eqn (3.13). The appropriate solution in region AB$\bar{B}$ is

$$\dot{\psi} = \Omega_-(\alpha_T - \theta_T). \tag{3.14}$$

Hence

$$\frac{\partial\dot{\psi}}{\partial\alpha_T} = -\frac{\partial\dot{\psi}}{\partial\theta_T}. \tag{3.15}$$

It also follows that $(\partial\dot{\psi}/\partial\theta_T)$ is constant along lines defined by $\alpha_T - \theta_T =$ constant, which implies that $(\partial\dot{\psi}/\partial\theta_T)$ along AB can be linked to $(\partial\dot{\psi}/\partial\theta_T)$ along A$\bar{B}$. We have

$$\frac{\partial\dot{\psi}}{\partial\theta_T}\left(s = s_1, \theta_T = \frac{1}{2}\kappa\pi\right) = \frac{\partial\dot{\psi}}{\partial\theta_T}\left(s = c_T, \theta_T = \frac{1}{2}\kappa\pi - \cos^{-1}\frac{c_T}{s_1}\right). \tag{3.16}$$

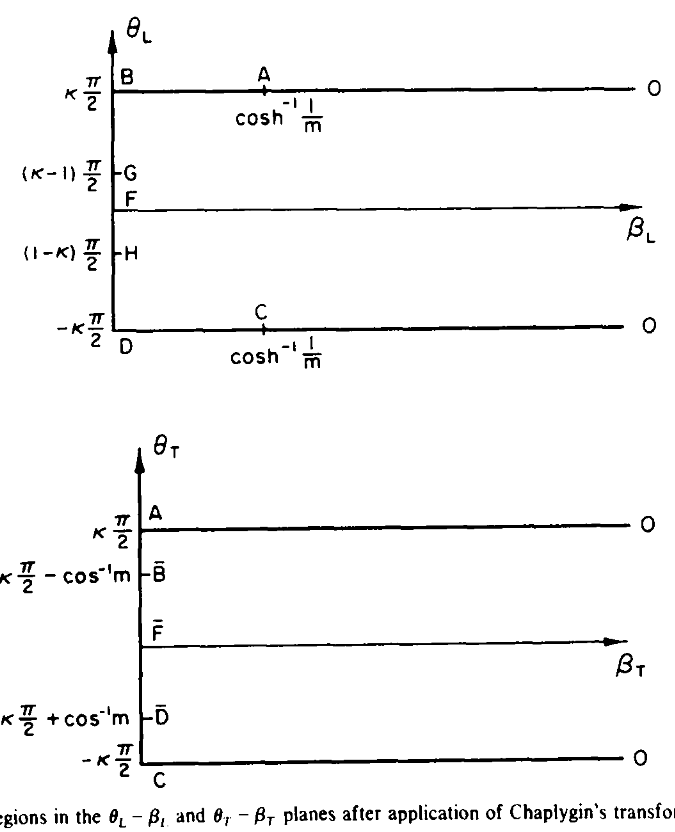

Fig. 2. Regions in the $\theta_L - \beta_L$ and $\theta_T - \beta_T$ planes after application of Chaplygin's transformation.

Similarly in region $CD\bar{D}$ we have

$$\dot{\psi} = \Omega_+(\alpha_T + \theta_T). \tag{3.17}$$

Hence

$$\frac{\partial\dot{\psi}}{\partial\alpha_T} = \frac{\partial\dot{\psi}}{\partial\theta_T}, \tag{3.18}$$

and $(\partial\dot{\psi}/\partial\theta_T)$ along CD is linked to $(\partial\dot{\psi}/\partial\theta_T)$ along by $C\bar{D}$ by

$$\frac{\partial\dot{\psi}}{\partial\theta_T}\left(s = s_1, \theta_T = -\frac{1}{2}\kappa\pi\right) = \frac{\partial\dot{\psi}}{\partial\theta_T}\left(s = c_T, \theta_T = -\frac{1}{2}\kappa\pi + \cos^{-1}\frac{c_T}{s_1}\right). \tag{3.19}$$

Along AB and CD we have $\tau_\theta = 0$ and $\tau_{\theta r} = 0$. By introducing the transformations (3.8) and (3.12) in eqns (3.6) and (3.7) we find

$$\frac{1 - 2m^2\cosh^2\beta_L}{m\sinh\beta_L}\frac{\partial\dot{\varphi}}{\partial\beta_L} + 2m\cosh\beta_L\frac{\partial\dot{\psi}}{\partial\theta_T} = 0 \tag{3.20}$$

$$-2m\cosh\beta_L\frac{\partial\dot{\varphi}}{\partial\theta_L} - \frac{1 - 2m^2\cosh^2\beta_L}{(1 - m^2\cosh^2\beta_L)^{1/2}}\frac{\partial\dot{\psi}}{\partial\alpha_T} = 0 \tag{3.21}$$

where

$$m = c_T/c_L. \tag{3.22}$$

Equations (3.20) and (3.21) can now be used together with eqns (3.15)–(3.19) to provide an equation containing $\dot{\varphi}$ only along the segments AB and CD, and an equation containing both $\dot{\varphi}$ and $\dot{\psi}$ along $A\bar{B}$ and $C\bar{D}$. The results are summarized in eqns (3.30) and (3.31).

The solutions to Laplace's equations in the strips, can be written as the real parts of analytic functions of the complex variables $\gamma_L = \beta_L + i\theta_L$ and $\gamma_T = \beta_T + i\theta_T$, i.e.

$$\dot{\varphi}(\beta_L, \theta_L) = Re[\Phi(\gamma_L)] \tag{3.23}$$

$$\dot{\psi}(\beta_T, \theta_T) = Re[\Psi(\gamma_T)]. \tag{3.24}$$

The boundary conditions of the strips can be summarized as follows:

Along $\bar{B}\bar{F}\bar{D}$, we have $\beta_T = 0$ and $-(1/2)\kappa\pi + \cos^{-1}m < \theta_T < (1/2)\kappa\pi - \cos^{-1}m$ and the boundary condition is

$$\dot{\psi} = 0. \tag{3.25}$$

Along BG and DH, we have $\beta_L = 0$ and $(1/2)\kappa\pi - (1/2)\pi < \theta_L < (1/2)\kappa\pi$ and $-(1/2)\kappa\pi < \theta_L < -(1/2)\kappa\pi + (1/2)\pi$, respectively, and the boundary condition is

$$\dot{\varphi} = -\tau_0/\rho. \tag{3.26}$$

Along HFG, we have $\beta_L = 0$ and $-(1/2)\kappa\pi + (1/2)\pi < \theta_L < (1/2)\kappa\pi - (1/2)\pi$ and the boundary condition is

$$\dot{\varphi} = 0. \tag{3.27}$$

Along OA and OC, the points are related by $\theta_T = \theta_L = \pm(1/2)\kappa\pi$ and $\cosh\beta_T = m\cosh\beta_L$ and we have

$$\frac{1 - 2m^2\cosh^2\beta_L}{m\sinh\beta_L}\frac{\partial\dot{\varphi}}{\partial\beta_L} + 2m\cosh\beta_L\frac{\partial\dot{\psi}}{\partial\theta_T} = 0 \tag{3.28}$$

$$\frac{1 - 2m^2\cosh^2\beta_L}{(m^2\cosh^2\beta_L - 1)^{1/2}}\frac{\partial\dot{\psi}}{\partial\beta_T} - 2m\cosh\beta_L\frac{\partial\dot{\varphi}}{\partial\theta_L} = 0. \tag{3.29}$$

Along AB (CD) and A$\bar{B}$ (C$\bar{D}$), the points on AB (CD) are defined by $\theta_L = \pm(1/2)\kappa\pi$, $\cosh\beta_L < 1/m$, while the corresponding points on A$\bar{B}$ (C$\bar{D}$) follow from

$$\beta_T = 0, \quad \theta_T = \pm\left[\frac{1}{2}\kappa\pi - \cos^{-1}(m\cosh\beta_L)\right],$$

where the + sign holds for AB and A$\bar{B}$, and the − sign holds for CD and C$\bar{D}$. The boundary conditions are

$$\frac{\partial\dot{\varphi}}{\partial\beta_L} \pm \frac{4m^3\cosh^2\beta_L\sinh\beta_L(1-m^2\cosh^2\beta_L)^{1/2}}{(1-2m^2\cosh^2\beta_L)^2}\frac{\partial\dot{\varphi}}{\partial\theta_L} = 0 \tag{3.30}$$

$$\frac{\partial\dot{\psi}}{\partial\theta_T} \mp \frac{2m\cosh\beta_L(1-m^2\cosh^2\beta_L)^{1/2}}{1-2m^2\cosh^2\beta_L}\frac{\partial\dot{\varphi}}{\partial\theta_L} = 0. \tag{3.31}$$

4. CONFORMAL MAPPING

It is not possible to obtain directly analytic functions $\Phi(\gamma_L)$ and $\Psi(\gamma_T)$, whose real parts satisfy the boundary conditions given by eqns (3.25)–(3.31). We will, therefore use a conformal mapping, to map the γ_L and γ_T-planes on the upper halves of complex $\zeta_L(=\xi_L + i\eta_L)$ and $\zeta_T(=\xi_T + i\eta_T)$-planes, respectively. The boundaries of the strips will be mapped on the real axes. Appropriate conformal mappings are

$$\frac{1}{\zeta_L} = \cosh\left(\frac{\gamma_L}{\kappa} - i\frac{\pi}{2}\right), \quad \frac{1}{\zeta_T} = \cosh\left(\frac{\gamma_T}{\kappa} - i\frac{\pi}{2}\right). \tag{4.1a,b}$$

The complex ζ_L- and ζ_T-planes, and the locations of the points on the real axes are shown in Figs. 3(a),(b).

In the ζ_L and ζ_T-planes we have

$$\dot{\varphi}(\xi_L, \eta_L) = Re[\Phi(\zeta_L)], \quad \dot{\psi}(\xi_T, \eta_T) = Re[\Psi(\zeta_T)]. \tag{4.2a,b}$$

The boundary conditions along the real axes of the ζ-planes can be obtained by elementary

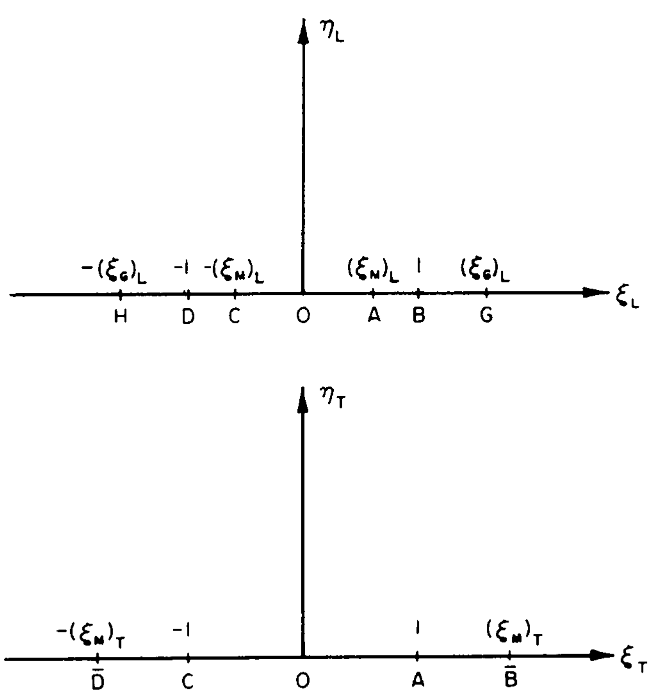

Fig. 3. Conformal mappings of strips on half planes.

manipulations which involve the transformation of derivatives in the γ-planes into derivatives in the ζ-planes. In these manipulations we use

$$\frac{d\zeta_L}{d\gamma_L} = \begin{cases} -\xi_L(1-\xi_L^2)^{1/2}/\kappa & \text{for} \quad \eta = 0, \quad |\xi_L| \leq 1 \\ i|\xi_L|(\xi_L^2-1)^{1/2}/\kappa & \text{for} \quad \eta = 0, \quad |\xi_L| \geq 1. \end{cases} \tag{4.3}$$

An analogous relation for $d\zeta_T/d\gamma_T$ can be written by replacing subscripts L by subscripts T. The boundary conditions are then obtained as:

Along OA and OC, we have $m \cosh[\kappa \cosh^{-1}(1/|\xi_L|)] = \cosh[\kappa \cosh^{-1}(1/|\xi_T|)]$, and the boundary conditions are

$$\xi_T(1-\xi_T^2)^{1/2}\frac{1-2m^2\cosh^2\beta_L}{(m^2\cosh^2\beta_L-1)^{1/2}}\frac{\partial\dot{\psi}}{\partial\xi_T} - \xi_L(1-\xi_L^2)^{1/2}2m\cosh\beta_L\frac{\partial\dot{\varphi}}{\partial\eta_L} = 0$$

$$\xi_L(1-\xi_L^2)^{1/2}\frac{1-2m^2\cosh^2\beta_L}{m\sinh\beta_L}\frac{\partial\dot{\varphi}}{\partial\xi_L} + \xi_T(1-\xi_T^2)^{1/2}2m\cosh\beta_L\frac{\partial\dot{\psi}}{\partial\eta_T} = 0. \tag{4.4}$$

Along AB and CD, we have $m \cosh[\kappa \cosh^{-1}(1/|\xi_L|)] = \cos[\kappa \cos^{-1}(1/|\xi_T|)]$, and the boundary conditions are

$$\frac{\partial\dot{\varphi}}{\partial\xi_L} \pm \frac{4m^3\cosh^2\beta_L\sinh\beta_L(1-m^2\cosh^2\beta_L)^{1/2}}{(1-2m^2\cosh^2\beta_L)^2}\frac{\partial\dot{\varphi}}{\partial\eta_L} = 0$$

$$|\xi_T|(\xi_T^2-1)^{1/2}\frac{\partial\dot{\psi}}{\partial\xi_T} \mp \xi_L(1-\xi_L^2)^{1/2}\frac{2m\cosh\beta_L(1-m^2\cosh^2\beta_L)^{1/2}}{1-2m^2\cosh^2\beta_L}\frac{\partial\dot{\varphi}}{\partial\eta_L} = 0. \tag{4.5}$$

In these equations the + sign holds for AB, while the − sign holds for CD. The second equation connects the fields along AB and A$\bar{\text{B}}$, and along CD and C$\bar{\text{D}}$. In eqns (4.4)–(4.5) the relation between β_L and ξ_L is given by

$$\cosh\beta_L = \cosh[\kappa\cosh^{-1}(1/|\xi_L|)]. \tag{4.6}$$

Along the remainder of the real axes we have:

$$\eta_L = 0, \quad |\xi_L| \geq 1: \quad \frac{\partial\dot{\varphi}}{\partial\xi_L} = \frac{\tau_0}{\rho}\{\delta[\xi_L - (\xi_G)_L] - \delta[\xi_L + (\xi_G)_L]\} \tag{4.7}$$

$$\eta_T = 0, \quad |\xi_T| \geq (\xi_M)_T: \quad \frac{\partial\dot{\psi}}{\partial\xi_T} = 0. \tag{4.8}$$

Expressions relating $|\xi_L|$ and $|\xi_T|$ are given above. The signs of corresponding ξ_L and ξ_T are the same, i.e.

$$\xi_T(\xi_L) = \text{sgn}(\xi_L)|\xi_T(|\xi_L|)|.$$

Let us define $\Gamma(\zeta_L) = d\Phi/d\zeta_L$. It can be shown that $\Gamma(\zeta_L)$ has zeros at $\xi_L = \pm\xi_0$, where

$$\xi_0 = [\cosh(\kappa^{-1}\cosh^{-1}(1/m\sqrt{2}))]^{-1}. \tag{4.9}$$

It is now convenient to define

$$\Gamma(\xi_L, 0) = \frac{\tau_0}{\rho}(\xi_0^2 - \xi_L^2)[\Gamma_1(\xi_L) + i\Gamma_2(\xi_L)]. \tag{4.10}$$

Similarly we define $\Omega(\zeta_T) = d\Psi/d\zeta_T$, and

$$\Omega(\xi_T, 0) = \frac{\tau_0}{\rho}[\Omega_1(\bar{\xi}_T) + i\Omega_2(\bar{\xi}_T)], \tag{4.11}$$

where

$$\bar{\xi}_T = \xi_T/(\xi_M)_T. \tag{4.12}$$

In terms of the functions defined by eqns (4.10) and (4.11), the relations given by (4.4)–(4.8) can be rewritten as

$$|\xi_L| \le (\xi_M)_L: \quad K_0(\xi_L)\Gamma_1(\xi_L) + K_1(\xi_L)\Omega_2(\bar{\xi}_T) = 0 \tag{4.13}$$

$$(\xi_M)_L \le |\xi_L| \le 1: \quad K_0(\xi_L)\Gamma_1(\xi_L) + K_2(\xi_L)\Gamma_2(\xi_L) = 0 \tag{4.14}$$

$$(\bar{\xi}_T) \le 1: \quad \Omega_1(\bar{\xi}_T) = K_3(\xi_L)\Gamma_2(\xi_L) \tag{4.15}$$

where

$$K_0(\xi_L) = [\xi_0^2 - \xi_L^2]^2 \tag{4.16}$$

$$K_1(\xi_L) = \frac{2(\xi_0^2 - \xi_L^2)m^2 \cosh\beta_L \sinh\beta_L}{2m^2\cosh\beta_L - 1} \frac{\xi_T(1-\xi_T^2)^{1/2}}{\xi_L(1-\xi_L^2)^{1/2}} \tag{4.17}$$

$$K_2(\xi_L) = \mp\frac{4(\xi_0^2 - \xi_L^2)^2 m^3 \cosh^2\beta_L \sinh\beta_L(1 - m^2\cosh^2\beta_L)^{1/2}}{(2m^2\cosh^2\beta_L - 1)^2} \tag{4.18}$$

$$K_3(\xi_L) = \frac{2(\xi_0^2 - \xi_L^2)m\cosh\beta_L(m^2\cosh^2\beta_L - 1)^{1/2}}{2m^2\cosh^2\beta_L - 1} \frac{\xi_L(1-\xi_L^2)^{1/2}}{\xi_T(1-\xi_T^2)^{1/2}}. \tag{4.19}$$

In addition, the relation between β_L and ξ_L is given by eqn (4.6), while the expressions relating ξ_L and ξ_T are stated preceding eqns (4.4) and (4.5). In eqn (4.18) the plus and minus signs hold for $\xi_L > 0$ and $\xi_L < 0$, respectively.

5. SINGULARITIES

Since the faces of the wedge are free of tractions, eqns (3.6) and (3.7) yield relations between the derivatives of $\dot{\varphi}$ and $\dot{\psi}$ at $\theta = \pm\kappa\pi/2$. By employing these relations to eliminate the derivatives of $\dot{\psi}$, and by using eqn (3.8), we obtain the following expressions for the particle velocities on the faces of the wedge

$$r\dot{u}_r = -\left[2m\frac{c_T}{s}\left(\frac{c_L^2}{s^2} - 1\right)^{1/2}\right]^{-1} \frac{\partial\dot{\varphi}}{\partial\beta_L} \tag{5.1}$$

$$r\dot{u}_\theta = (1 - 2c_T^2/s^2)^{-1}\frac{\partial\dot{\varphi}}{\partial\theta_L}. \tag{5.2}$$

Next $\partial\dot{\varphi}/\partial\beta_L$ and $\partial\dot{\varphi}/\partial\theta_L$ can be expressed in terms of $\Gamma_1(\xi_L)$ and $\Gamma_2(\xi_L)$ by using eqns (4.3) and (4.10), and the particle velocities can be rewritten as

$$r\dot{u}_r = \frac{\tau_0}{\rho}\frac{s^2(\xi_0^2 - \xi_L^2)}{2m^2 c_L(c_L^2 - s^2)^{1/2}} \frac{\xi_L(1-\xi_L^2)^{1/2}}{\kappa}\Gamma_1(\xi_L) \tag{5.3}$$

$$r\dot{u}_\theta = -\frac{\tau_0}{\rho}\frac{s^2(\xi_0^2 - \xi_L^2)}{2c_T^2 - s^2}\frac{\xi_L(1-\xi_L^2)^{1/2}}{\kappa}\Gamma_2(\xi_L). \tag{5.4}$$

Since $r\partial/\partial t = -s^2\partial/\partial s$, it follows from eqn (5.4) that near the vertex of the wedge, i.e. for small values of both s and ξ_L, we have

$$\xi_L\Gamma_2(\xi_L)|_{\xi_L\to 0} \propto \left.\frac{\partial u_\theta}{\partial s}\right|_{s\to 0}. \tag{5.5}$$

In Appendix A it has been shown that $u_\theta \propto s^p$ as $s \to 0$, where p is the solution of eqn (A10). For small s and small ξ_L, the conformal mapping given by eqns (4.1a,b) yields $s \propto |\xi_L|^\kappa$. Combining the result we find

$$\Gamma_2(\xi_L)|_{\xi_L \to 0} \propto |\xi_L|^{-q}, \quad q = -\kappa(p-1)+1. \tag{5.6}$$

In addition to singularities at the vertex, the functions $\Gamma_1(\xi_L)$ and $\Gamma_2(\xi_L)$ have singularities at the points G and H, where the plane waves are matched to the cylindrical waves, see Fig. 1. Moreover, we expect singularities at points $s = c_R$, i.e. at the points propagating with the velocity of Rayleigh waves. It is assumed that $\Gamma_2(\xi_L)$ and $\Omega_1(\bar{\xi}_T)$ have simple poles at these points, which implies that $\Gamma_1(\xi_L)$ and $\Omega_2(\bar{\xi}_T)$ contain Dirac delta functions. In the sequel it will be shown that the singularities at $s = c_R$ are compatible with the system of governing integral equations. For the limit case of $\kappa = 2$, which corresponds to a crack in an unbounded medium, an analytical solution can be obtained, and the presence of these singularities can be verified.

In Appendix B it is shown how to construct an analytic function $\Gamma^*(\zeta_L)$ whose real part vanishes on the real axis for $|\xi_L| \ge 1$, and whose imaginary part has the singular behavior on the real axis shown by eqn (5.6). On the real axis this function is

$$\Gamma^*(\xi_L) = \Gamma_1^\dagger(\xi_L) + i\Gamma_2^\dagger(\xi_L), \tag{5.7}$$

where

$$\Gamma_1^\dagger(\xi_L) = \begin{cases} \operatorname{sgn}(\xi_L)|\xi_L|^{-q}(1-\xi_L^2)^{1/2} \sin\frac{q\pi}{2}; & |\xi_L| \le 1 \\ 0 & ; \ |\xi_L| \ge 1 \end{cases} \tag{5.8}$$

$$\Gamma_2^\dagger(\xi_L) = \begin{cases} \frac{1}{q\pi}\mathscr{B}\left(\frac{1}{2},\frac{2-q}{2}\right)\sin\left(\frac{q\pi}{2}\right)F\left(1,\frac{q-1}{2};\frac{q+2}{2};\xi_L^2\right) - |\xi_L|^{-q}(1-\xi_L^2)^{1/2}\cos\left(\frac{q\pi}{2}\right); & |\xi_L| \le 1 \\ \frac{1}{\pi}\frac{1}{\xi_L^2}\mathscr{B}\left(\frac{1}{2},\frac{2-q}{2}\right)\sin\left(\frac{q\pi}{2}\right)F\left(\frac{2-q}{2},1;\frac{1}{2};\frac{\xi_L^2-1}{\xi_L^2}\right) - |\xi_L|^{-q}(\xi_L^2-1)^{1/2}\sin\left(\frac{q\pi}{2}\right); & |\xi_L| \ge 1. \end{cases} \tag{5.9}$$

In eqns (5.8) and (5.9) $\mathscr{B}(.,.)$ is the Beta function, and $F(.,.;.;.)$ is the "ordinary" Hypergeometric function[13]. Similarly an analytic function $\Omega^*(\bar{\xi}_T)$ can be constructed, so that the imaginary part vanishes on the real axis for $|\bar{\xi}_T| \ge 1$, and the real part shows the singular behavior on the real axis given by eqn (5.6). This function is

$$\Omega^*(\bar{\xi}_T) = \Omega_1^\dagger(\bar{\xi}_T) + i\Omega_2^\dagger(\bar{\xi}_T), \tag{5.10}$$

where

$$\Omega_1^\dagger(\bar{\xi}_1) = \begin{cases} \Gamma_2^\dagger(\bar{\xi}_T)(1-\bar{\xi}_T^2)^{1/2}; & |\bar{\xi}_T| \le 1 \\ 0; & |\bar{\xi}_T| \ge 1 \end{cases} \tag{5.11}$$

$$\Omega_2^\dagger(\xi_T) = \begin{cases} -\Gamma_1^\dagger(\bar{\xi}_T)(1-\bar{\xi}_T^2)^{1/2}; & |\bar{\xi}_T| \le 1 \\ -\Gamma_2^\dagger(\bar{\xi}_T)\operatorname{sgn}(\bar{\xi}_T)(\bar{\xi}_T^2-1)^{1/2}; & |\bar{\xi}_T| \ge 1. \end{cases} \tag{5.12}$$

6. METHOD OF SOLUTION

The solution of the system of eqns (4.13)–(4.15) will be obtained by separating the singular parts of $\Gamma_1(\xi_L)$ and $\Omega_1(\bar{\xi}_T)$, and by expanding the non-singular parts in terms of Chebyshev polynomials of the second kind. On the basis of the observations on the singularities, stated in Section 5, $\Gamma_1(\xi_L)$ can be expressed in the following form

$$\Gamma_1(\xi_L) = (1-\xi_L^2)^{1/2}\sum_{i=1}^{N} P_i U_{2i-1}(\xi_L) + B\Gamma_1^\dagger(\xi_L) + A\pi\{\delta[\xi_L - (\xi_R)_L] - \delta[\xi_L + (\xi_R)_L]\}$$
$$+ [\xi_0^2 - (\xi_G)_L^2]^{-1}\{\delta[\xi_L - (\xi_G)_L] - \delta[\xi_L + (\xi_G)_L]\}. \tag{6.1}$$

Where $U_{2i-1}(\xi_L)$ are Chebyshev polynomials of the second kind, and P_i, A and B are as yet unknown constants. The function $\Gamma_2(\xi_L)$ can be obtained by writing the Hilbert transform of the non-singular parts of $\Gamma_1(\xi_L)$, and by adding the parts corresponding to the remaining terms in eqn (6.1). These are poles corresponding to the delta functions, and $\Gamma_2^\dagger(\xi_L)$ corresponding to $\Gamma_1^\dagger(\xi_L)$. Thus we obtain

$$\Gamma_2(\xi_L) = \sum_{i=1}^{N} P_i T_{2i}(\xi_L) + B\Gamma_2^\dagger(\xi_L) + A\frac{2(\xi_R)_L}{\xi_L^2 - (\xi_R)_L^2} + \frac{1}{\xi_L^2 - (\xi_G)_L^2}\frac{2(\xi_G)_L}{\pi[\xi_0^2 - (\xi_G)_L^2]}. \tag{6.2}$$

In this equation $T_{2i}(\xi_L)$ is the Chebyshev polynominal of the first kind. The pertinent relations between $U_{2i-1}(\xi_L)$ and $T_{2i}(\xi_L)$, via the Hilbert transform, are given in Ref. [12].

For $|\bar{\xi}_T| \le 1$, $\Omega_1(\bar{\xi}_T)$ is related to $\Gamma_2(\xi_L)$ by eqn (4.15), while $\Omega_1(\bar{\xi}_T) \equiv 0$ for $|\bar{\xi}_T| \ge 1$. The singularities of $\Omega_1(\bar{\xi}_T)$ are, therefore, of the same kind as those of $\Gamma_2(\xi_L)$. The singular nature at the points defined by $s = c_R$ can be expressed by

$$\Lambda(\bar{\xi}_T) = \Lambda_1(\bar{\xi}_T) + i\Lambda_2(\bar{\xi}_T) \tag{6.3}$$

where

$$\Lambda_1(\bar{\xi}_T) = \begin{cases} \dfrac{2(\bar{\xi}_R)_T(1-\bar{\xi}_T^2)^{1/2}}{\bar{\xi}_T^2 - (\bar{\xi}_R)_T^2}; & |\bar{\xi}_T| \le 1 \\ 0; & |\bar{\xi}_T| \ge 1 \end{cases} \tag{6.4}$$

$$\Lambda_2(\bar{\xi}_T) = \begin{cases} -\pi[1-(\bar{\xi}_R)_T^2]^{1/2}\{\delta[\bar{\xi}_T - (\bar{\xi}_R)_T] - \delta[\bar{\xi}_T + (\bar{\xi}_R)_T]\}; & |\bar{\xi}_T| \le 1 \\ -\dfrac{2(\bar{\xi}_R)_T(\bar{\xi}_T^2 - 1)^{1/2}\,\mathrm{sgn}\,(\bar{\xi}_T)}{\bar{\xi}_T^2 - (\bar{\xi}_R)_T^2}; & |\bar{\xi}_T| \ge 1. \end{cases} \tag{6.5}$$

The function $\Omega_1(\bar{\xi}_T)$ can then be expressed as

$$\Omega_1(\bar{\xi}_T) = (1-\bar{\xi}_T^2)^{1/2}\sum_{i=1}^{M} Q_i U_{2i-2}(\bar{\xi}_T) + AC\Lambda_1(\bar{\xi}_T) + BD\Omega_1^\dagger(\bar{\xi}_T). \tag{6.6}$$

Here $\Omega_1^\dagger(\bar{\xi}_T)$ represents the singular behavior at the vertex. It follows that $\Omega_2(\bar{\xi}_T)$ is of the form

$$\Omega_2(\bar{\xi}_T) = \sum_{i=1}^{M} Q_i T_{2i-1}(\bar{\xi}_T) + AC\Lambda_2(\bar{\xi}_T) + BD\Omega_2^\dagger(\bar{\xi}_T). \tag{6.7}$$

We are now ready to substitute the expressions for $\Gamma_2(\xi_L)$, see eqn (6.2), and $\Omega_1(\bar{\xi}_T)$, see eqn (6.6), into eqn (4.15). The resulting equation first yields expressions for C and D, by the requirement that the contributions at the singular points in the range $|\bar{\xi}_T| \le 1$ from $\Gamma_2(\xi_L)$ and $\Omega_1(\bar{\xi}_T)$, respectively, must cancel each other. We find

$$C = \left[\frac{K_3(\xi_L)}{(1-\bar{\xi}_T^2)^{1/2}}\frac{d\bar{\xi}_T}{d\xi_L}\right]_{\xi_L \to (\xi_R)_L} \tag{6.8}$$

$$D = \left[\frac{K_3(\xi_L)}{(1-\bar{\xi}_T^2)^{1/2}}\left(\frac{\bar{\xi}_T}{\xi_L}\right)^q\right]_{\xi_L \to 0}. \tag{6.9}$$

Next the same equation can be used to express the coefficients Q_j in terms of P_i, A, B, C and D by multiplying the equation by $(2/\pi)\ U_{2j-2}(\bar{\xi}_T)$, and integrating over $\bar{\xi}_T$ in the range $(-1, 1)$. The result is

$$Q_j = \sum_{i=1}^{N} P_i a_{ij} + Ab_j + Bc_j + d_j \quad j = 1, 2, \ldots, M \tag{6.11}$$

where

$$a_{ij} = \frac{2}{\pi}\int_{-1}^{1} T_{2i}(\xi_L)K_3(\xi_L)U_{2j-2}(\bar{\xi}_T)\,\mathrm{d}\bar{\xi}_T \tag{6.12}$$

$$b_j = \frac{2}{\pi}\int_{-1}^{1}\left[\frac{2(\xi_R)_L K_3(\xi_L)}{\xi_L^2-(\xi_R)_L^2} - C\Lambda_1(\bar{\xi}_T)\right]U_{2j-2}(\bar{\xi}_T)\,\mathrm{d}\bar{\xi}_T \tag{6.13}$$

$$c_j = \frac{2}{\pi}\int_{-1}^{1}[\Gamma_2^*(\xi_L)K_3(\xi_L) - D\Omega_1^*(\bar{\xi}_T)]U_{2j-2}(\bar{\xi}_T)\,\mathrm{d}\bar{\xi}_T \tag{6.14}$$

$$d_j = \frac{2(\xi_G)_L}{\pi[\xi_0^2-(\xi_G)_L^2]}\frac{2}{\pi}\int_{-1}^{1}\frac{K_3(\xi_L)}{\xi_L^2-(\xi_G)_L^2}U_{2j-2}(\bar{\xi}_T)\,\mathrm{d}\bar{\xi}_T. \tag{6.15}$$

The integrals in eqns (6.12)–(6.15) can be evaluated using quadrature formulas.

Equation (4.13) and (4.14) can be combined into one equation in the range $|\xi_L| \le 1$, by defining $K_1(\xi_L) \equiv 0$ for $(\xi_M)_L \le |\xi_L| \le 1$, and $K_2(\xi_L) \equiv 0$ for $|\xi_L| \le (\xi_M)_L$. The expressions for $\Gamma_1(\xi_L)$, $\Gamma_2(\xi_L)$ and $\Omega_2(\bar{\xi}_T)$, given by eqns (6.1), (6.2) and (6.4), respectively, can then be substituted. In the resulting equation, which holds in the range $|\xi_L| \le 1$, the δ-functions at the Rayleigh points cancel each other identically. The terms representing the singular behavior at the vertex also cancel at the point corresponding to the vertex. These results show the compatibility of the chosen singularities with the system of equations. Next the Q_j's, given by eqn (6.11) are substituted in the equation formed by combining (4.13) and (4.14). The resulting equation is multiplied by $(2/\pi)U_{2k-1}(\xi_L)$, and the product terms are integrated over ξ_L in the range $(-1, 1)$. This results in the following system of equations

$$\sum_{i=1}^{N} P_i e_{ik} + Af_k + Bg_k + h_K = 0. \quad k = 1, 2, \ldots, N \tag{6.16}$$

where

$$e_{ik} = \frac{2}{\pi}\int_{-1}^{1}[K_0(\xi_L)U_{2i-1}(\xi_L)(1-\xi_L^2)^{1/2} + K_1(\xi_L)\sum_{j=1}^{M} a_{ij}T_{2j-1}(\bar{\xi}_T) + K_2(\xi_L)T_{2i}(\xi_L)]U_{2k-1}(\xi_L)\,\mathrm{d}\xi_L \tag{6.17}$$

$$f_k = \frac{2}{\pi}\int_{-1}^{1}\left[K_1(\xi_L)\sum_{j=1}^{M} b_j T_{2j-1}(\bar{\xi}_T) + \frac{2(\xi_R)_L K_2(\xi_L)}{\xi_L^2-(\xi_R)_L^2}\right]\cdot U_{2k-1}(\xi_L)\,\mathrm{d}\xi_L \tag{6.18}$$

$$g_k = \frac{2}{\pi}\int_{-1}^{1}\left[K_0(\xi_L)\Gamma_1^*(\xi_L) + K_1(\xi_L)\left\{\Omega_2^*(\bar{\xi}_T) + \sum_{j=1}^{M} c_j T_{2j-1}(\bar{\xi}_T)\right\} + K_2(\xi_L)\Gamma_2^*(\xi_L)\right]U_{2k-1}(\xi_L)\,\mathrm{d}\xi_L \tag{6.19}$$

$$h_k = \frac{2}{\pi}\int_{-1}^{1}\left[K_1(\xi_L)\sum_{j=1}^{M} d_j T_{2j-1}(\bar{\xi}_T) + \frac{2(\xi_G)_L}{\pi[\xi_0^2-(\xi_G)_L^2]}\cdot\frac{K_2(\xi_L)}{\xi_L^2-(\xi_G)_L^2}\right]U_{2k-1}(\xi_L)\,\mathrm{d}\xi_L. \tag{6.20}$$

Equation (6.16) represents a system of N equation in $(N+2)$ unknowns. Thus, two additional equations are needed to complete the formulation. These equations are obtained by observing that the analytic functions $\Phi(\zeta_L)$ and $\Psi(\zeta_T)$ should vanish uniformly at infinity in upper half planes. The required relations can be obtained by considering the behavior of $\Gamma(\zeta_L)$ and $\Omega(\zeta_T)$ along the real axis. On the basis of eqn (4.10), we conclude $\Gamma_2(\xi_L) = O(\xi_L^{-2-d_1})$ as $|\xi_L| \to \infty$, where $d_1 > 1$, while eqn (4.11) yields $\Omega_2(\bar{\xi}_T) = O(\bar{\xi}_T^{-d_2})$ as $|\bar{\xi}_T| \to \infty$, where $d_2 > 1$. Thus in the expansions of $\Gamma_2(\xi_L)$ the coefficient of $1/\xi_L^2$ must vanish, while in the expansion of $\Omega_2(\bar{\xi}_T)$, the coefficient of $1/\bar{\xi}_T$ must vanish. Then, using eqns (6.2) we obtain

$$P_1 + 8(\xi_R)_L A + \frac{4B\sin(q\pi/2)}{\pi(3-q)}\mathscr{B}\left(\frac{1}{2}, \frac{2-q}{2}\right) + \frac{8}{\pi}\frac{(\xi_G)_L}{\xi_0^2-(\xi_G)_L^2} = 0 \tag{6.21}$$

Similarly, eqn (6.4) yields

$$\sum_{i=1}^{N} P_i a_{i1} + A[b_1 - 4(\bar{\xi}_R)_T C] + \left[c_1 - \frac{2D\sin(q\pi/2)}{\pi(3-q)}\mathcal{B}\left(\frac{1}{2}, \frac{2-q}{2}\right)\right] B + d_1 = 0. \tag{6.22}$$

Equations (6.16), (6.21) and (6.22) represent a system of $N+2$ simultaneous linear algebraic equations in $N+2$ unknowns, namely, P_i ($i = 1, \ldots, N$), A and B. The system can be solved on a digital computer using standard library routines.

7. STRESS INTENSITY FACTOR

At the vertex of the wedge, a stress intensity factor K for the circumferential stress, may be defined as

$$K = \lim_{s\to 0}\left\{\left[\frac{t\tau_\theta(s,\theta)}{\tau_0}\left(\frac{s}{c_T}\right)^{1-p}\right]_{\theta=0}\right\}. \tag{7.1}$$

In Appendix A, the circumferential particle velocity on the faces of the wedge is expressed in terms of K, see eqn (A13). Here we will use eqn (A13) to compute K.

An expression for $r\dot{u}_\theta/s^2$ (which equals $-\partial u_\theta/\partial s$) is given by eqn (5.4). Near the vertex of the wedge, i.e. for $\xi_L \to 0$, we find

$$\left.\frac{\partial u_\theta}{\partial s}\right|_{\theta=\kappa\pi/2} \sim \frac{\tau_0}{2\mu}\frac{\xi_0^2}{\kappa}\xi_L\Gamma_2(\xi_L). \tag{7.2}$$

Equations (5.9) and (6.2) give for $\xi_L \to 0$

$$\xi_L\Gamma_2(\xi_L) \sim -B|\xi_L|^{1-q}\cos(\pi q/2). \tag{7.3}$$

From the mapping defined by eqn (4.1a) we obtain near the vertex

$$\xi_L \sim 2\left(\frac{m}{2}\right)^{1/\kappa}\left(\frac{s}{c_T}\right)^{1/\kappa}. \tag{7.4}$$

Thus, eqn (7.2) can be rewritten as

$$\left.\frac{\partial u_\theta}{\partial s}\right|_{\theta=\kappa\pi/2} \sim -\frac{\tau_0}{2\mu}\frac{\xi_0^2}{\kappa}(2^{\kappa-1}m)^{p-1}B\cos\left(\frac{\pi q}{2}\right)\left(\frac{s}{c_T}\right)^{p-1} \tag{7.5}$$

where the relation $q = -\kappa(p-1)+1$ has also been used. Comparing eqns (7.5) and (A13) we conclude

$$K = -B\frac{\xi_0^2(1-p)(1-m^2)}{\kappa(2^{\kappa-1}m)^{1-p}}\frac{\sin(\kappa\pi/2)\sin(p\kappa\pi/2)\cos(q\pi/2)}{\sin[(1+p)\kappa\pi/2]\cos[(1-p)\kappa\pi/2]}. \tag{7.6}$$

8. RESULTS

In this paper we are particularly interested in the nature and the strength of stress singularities at the vertex of the wedge. In general, these stress singularities are of the form $(s/c_T)^{p-1}$. For the in-plane problem with stress boundary conditions, which is considered in this paper, the singularity of τ_θ follows from eqn (7.1), where p is the solution of eqn (A10). For a wedge subjected to surface tractions of the form $\tau_{\theta z} = \tau_0\delta(t)$, the shear stress $\tau_{\theta z}$ near the vertex is given by eqn (35) of [11]. For this case of antiplane strain we have $p = 1/\kappa$. For in-plane mixed conditions defined by $\tau_\theta = -\tau_0\delta(t)$ and $u_r = 0$ at $\theta = \pm\kappa\pi/2$, the singularity at the vertex can be analyzed by the method discussed in Appendix A. The coefficient p then is the solution of $\cos[(p+1)\kappa\pi/2]\cos[(p-1)\kappa\pi/2] = 0$, and we find for the lowest physical acceptable root $p = 3/\kappa - 1$. the singularity factors $p-1$ for the three cases discussed above, are

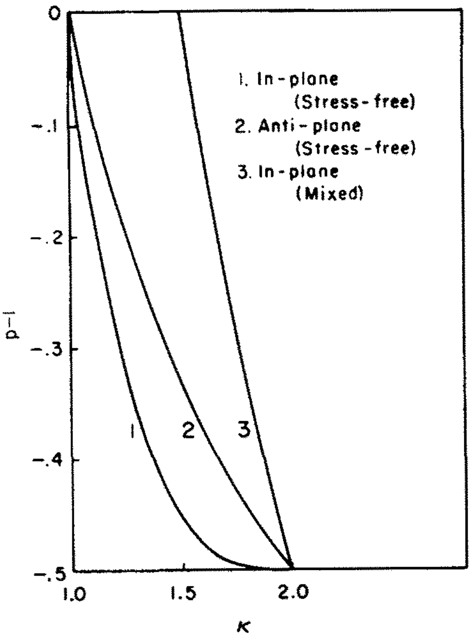

Fig. 4.

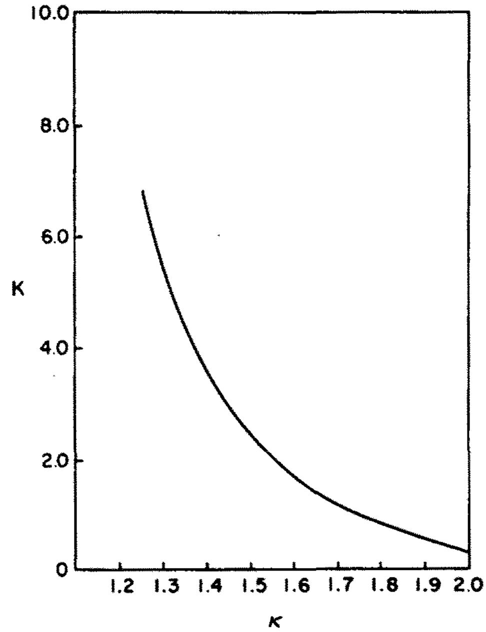

Fig. 5.

Fig. 4. Singularity coefficients for three loading conditions.

Fig. 5. Elastodynamic stress intensity factor versus the wedge angle.

plotted versus κ in Fig. 4. It is noted that the stress singularity is strongest for the case examined in this paper, for which the surface tractions are defined by eqns (2.5) and (2.6).

The elastodynamic stress intensity factor defined by eqn (7.1) is plotted in Fig. 5, for various values of the wedge angle. It is noteworthy that K decreases as κ approaches $\kappa = 2$, at least in the range of κ considered here. The case $\kappa = 2$ corresponds to a crack in an unbounded solid. The singularity disappears altogether as $\kappa = 1$ in the limit. For κ slightly larger than unity the method of computation used in this paper shows some instabilities, which indicates that a separate approach is needed to consider the limitcase $\kappa \to 1$. It is of interest to list the corresponding K's for antiplane strain, and for mixed conditions. For antiplane strain, i.e. $\tau_{\theta z} = \tau_0\delta(t)$ at $\theta = \pm\kappa\pi/2$, we find from [11]

$$K = \frac{4}{\pi\kappa}\left(\frac{1}{2}\right)^{1/\kappa} \sin(\pi/2\kappa) \tag{8.1}$$

For mixed conditions, i.e. $\tau_\theta = \tau_0\delta(t)$ and $u_r = 0$ at $\theta = \pm\kappa\pi/2$, we find

$$K = \frac{4}{\pi\kappa} m^{1/\kappa} 2^{1-3/\kappa}\{1 - m^{2/\kappa}[3 - 4\cos^2(\pi/2\kappa)]\}\cos(\pi/2\kappa). \tag{8.2}$$

The stress intensity factor for antiplane strain decreases as κ increases from one to two, while the stress intensity factor for the mixed conditions increases with increasing κ in that range.

Acknowledgement—The work reported here was carried out in the course of research sponsored by the National Science Foundation under Grant No. ENG 70-01465 A02 to Northwestern University.

REFERENCES

1. L. Knopoff, Elastic wave propagation in a wedge. *Wave Propagation in Solids* (Edited by J. Miklowitz). The American Society of Mechanical Engineers, New York (1969).
2. B. V. Kostrov, Diffraction of a plane wave by a smooth rigid wedge in an unbounded elastic medium in absence of friction. *Applied Mathematics and Mechanics* (PMM) **30**, 244 (1966).
3. S. H. Zemell, Diffraction of elastic waves by a rigid-smooth wedge. *SIAM J. of Appl. Math.* **29**, 582 (1975).

4. S. M. Kapustianskii, On an exact solution of the problem of elastic wave diffraction by a wedge. *Applied Mathematics and Mechanics* (PMM) **40**, 190 (1976).
5. M. Ziv, SBC quater plane subjected to a transient P wave and its diffraction at grazing incidence. *J. Acoust. Soc. America* **60**, 9 (1976).
6. J. D. Achenbach, *Wave Propagation in Elastic Solids*. North-Holland/American Elsevier, Amsterdam/New York (1973).
7. J. W. Miles, Honogeneous solutions in elastic wave propagation. *Quart. Appl. Math.* **XVIII**, 37 (1960).
8. J. C. Thompson and A. R. Robinson, *Exact Solutions of Some Dynamic Problems of Indentation and Transient Loadings of an Elastic Half-Space*. Civil Eng. Studies, Structural Res. Ser. No. 350, Univ. of Illinois, Urbana (1969).
9. J. R. Willis, Self-similar problems in elastodynamics, *Phil. Trans. Roy. Soc.* (London) **274**, 435 (1973).
10. G. P. Cherepanov and E. F. Afansev, Some dynamic problems of the theory of elasticity-A review. *Int. J. Engng Sci.* **12**, 665 (1974).
11. J. D. Achenbach, Shear waves in an elastic wedge. *Int. J. Solids Structures* **6**, 379 (1970).
12. F. Erdogan, G. D. Gupta and T. S. Cook, Numerical solution of singular integral equations. *Methods of Analysis and Solutions of Crack Problems* (Edited by G. C. Sih). Noordhoff, Leyden (1973).
13. I. N. Sneddon, *Special Functions of Mathematical Physics and Chemistry*. Oliver and Boyd, Edinburgh (1956).
14. S. N. Karp and F. C. Karal, Jr., The elastic-field behavior in the neighborhood of a crack of arbitrary angle. *Communications on Pure and Applied Mathematics* **XV**, 413 (1962).

APPENDIX A

Asymptotic behavior at the vertex

For elastostatic problems the elastic-field behavior in the neighborhood of the vertex of a wedge-shaped void was analyzed by Karp and Karal[14]. In this appendix we follow essentially the same procedure for a self-similar elastodynamic field.

Introducting $s = r/t$ in the elastodynamic displacement equations of motion in polar coordinates, we obtain

$$c_L^2\frac{\partial}{\partial s}\left[\frac{\partial u_r}{\partial s}+\frac{u_r}{s}+\frac{1}{s}\frac{\partial u_\theta}{\partial \theta}\right]-c_T^2\frac{1}{s}\frac{\partial}{\partial \theta}\left[\frac{\partial u_\theta}{\partial s}+\frac{u_\theta}{s}-\frac{1}{s}\frac{\partial u_r}{\partial \theta}\right]=\frac{\partial}{\partial s}\left[s^2\frac{\partial u_r}{\partial s}\right] \tag{A1}$$

$$c_L^2\frac{1}{s}\frac{\partial}{\partial \theta}\left[\frac{\partial u_r}{\partial s}+\frac{u_r}{s}+\frac{1}{s}\frac{\partial u_\theta}{\partial \theta}\right]+c_T^2\frac{\partial}{\partial s}\left[\frac{\partial u_\theta}{\partial s}+\frac{u_\theta}{s}-\frac{1}{s}\frac{\partial u_r}{\partial \theta}\right]=\frac{\partial}{\partial s}\left[s^2\frac{\partial u_\theta}{\partial s}\right]. \tag{A2}$$

The stress components are

$$\frac{t\tau_\theta}{\mu}=\frac{1}{m^2}\left[\frac{\partial u_r}{\partial s}+\frac{1}{s}\frac{\partial u_\theta}{\partial \theta}+\frac{u_r}{s}\right]-2\frac{\partial u_r}{\partial s} \tag{A3}$$

$$\frac{t\tau_{\theta r}}{\mu}=\frac{1}{s}\frac{\partial u_r}{\partial \theta}+\frac{\partial u_\theta}{\partial s}-\frac{u_\theta}{s}, \tag{A4}$$

where m^2 is defined by eqn (3.22) as $m^2 = c_T^2/c_L^2$.

For the problems considered in this paper, the displacement components depend on s only. We then assume that for sufficiently small s, i.e. in the immediate vicinity of the vertex, the leading terms of the displacement components are of the forms

$$u_r(s,\theta) = s^p f(\theta) \tag{A5}$$

$$u_\theta(s,\theta) = s^p g(\theta). \tag{A6}$$

Substituting for u_r and u_θ in eqns (A1) and (A2), and retaining terms of order s^{p-2} only, we find two coupled ordinary differential equations for $f(\theta)$ and $g(\theta)$. Except for different symbols for m^2 and p, these equations are just the same as eqns (7) and (8) of Ref. [14]. Appropriate solutions for $f(\theta)$ and $g(\theta)$, which correspond to symmetric displacements relative to $\theta = 0$, i.e. $u_r(s,\theta) = u_r(s,-\theta)$, and $u_\theta(r,\theta) = -u_\theta(r,-\theta)$, are

$$f(\theta) = A\cos(1+p)\theta + C\cos(1-p)\theta \tag{A7}$$

$$g(\theta) = -A\sin(1+p)\theta - \nu C\sin(1-p)\theta \tag{A8}$$

where A and C are unknown constants, and

$$\nu = \frac{m^2(1-p)+(1+p)}{(1-p)+m^2(1+p)}. \tag{A9}$$

The stresses τ_θ and $\tau_{\theta r}$ can now be expressed in terms of $f(\theta)$ and $g(\theta)$ by using eqns (A3)–(A8). These expressions contain p as a still unknown parameter. Now we introduce the condition that the stresses τ_θ and $\tau_{\theta r}$ vanish on the faces of the wedge, i.e. at $\theta = \pm\kappa\pi/2$. This condition yields two algebraic equations for A and C. The requirement that the determinant of the coefficients must vanish results in the following equation relating p and κ:

$$\frac{\sin p\kappa\pi}{p\kappa\pi}+\frac{\sin\kappa\pi}{\kappa\pi}=0 \tag{A10}$$

At the vertex of the wedge, a stress intensity factor K for the circumferential stress is defined by eqn (7.1). By using

(A3) and (A5)–(A8), we find after eliminating C in favor of A

$$K = -\frac{4p\kappa A}{\tau_0(c_T)^{1-p}}\frac{\sin(\kappa\pi/2)\sin(p\kappa\pi/2)}{\cos[(1-p)\kappa\pi/2]}. \tag{A11}$$

Another useful expression is $\partial u_\theta/\partial s$ on the face of the wedge, which is defined by $\theta = \kappa\pi/2$. Near the vertex we find

$$\left.\frac{\partial u_\theta}{\partial s}\right|_{\theta=\kappa\pi/2} \sim -\frac{2As^{p-1}}{(1-p)(1-m^2)}\sin[(1+p)\kappa\pi/2]. \tag{A12}$$

Eliminating A from eqns (A11) and (A12) we obtain

$$\left.\frac{\partial u_\theta}{\partial s}\right|_{\theta=\kappa\pi/2} \sim \frac{K\tau_0/\mu}{(1-p)(1-m^2)}\frac{\sin[(1+p)\kappa\pi/2]\cos[(1-p)\kappa\pi/2]}{2\sin(\kappa\pi/2)\sin(p\kappa\pi/2)}\left(\frac{s}{c_T}\right)^{p-1}. \tag{A13}$$

APPENDIX B

Analytic functions with prescribed singularities

Let us first consider an analytic function $\chi(\zeta_L)$ of the form

$$\chi(\zeta_L) = -i(1-\zeta_L^2)^{1/2}(\zeta_L e^{-i\pi/2})^{-q}. \tag{B1}$$

On the real axis we have

$$\chi(\xi_L) = \chi_1(\xi_L) + i\chi_2(\xi_L) \tag{B2}$$

where

$$\chi_1(\xi_L) = \begin{cases} \operatorname{sgn}(\xi_L)|\xi_L|^{-q}(1-\xi_L^2)^{1/2}\sin\left(\frac{q\pi}{2}\right); & |\xi_L| \le 1 \\ -\operatorname{sgn}(\xi_L)|\xi_L|^{-q}(\xi_L^2-1)^{1/2}\cos\left(\frac{q\pi}{2}\right); & |\xi_L| \ge 1 \end{cases} \tag{B3}$$

$$\chi_2(\xi_L) = \begin{cases} -|\xi_L|^{-q}(1-\xi_L^2)^{1/2}\cos\left(\frac{q\pi}{2}\right); & |\xi_L| \le 1 \\ -|\xi_L|^{-q}(\xi_L^2-1)^{1/2}\sin\left(\frac{q\pi}{2}\right); & |\xi_L| \ge 1. \end{cases} \tag{B4}$$

Next we consider another analytic function $\chi^*(\zeta_L)$, such that, on the real axis we have

$$\chi^*(\xi_L) = \chi_1^*(\xi_L) + i\chi_2^*(\xi_L) \tag{B5}$$

where

$$\chi_1^*(\xi_L) = \begin{cases} 0; & |\xi_L| \le 1 \\ -\operatorname{sgn}(\xi_L)|\xi_L|^{-q}(\xi_L^2-1)^{1/2}\cos\left(\frac{q\pi}{2}\right); & |\xi_L| \ge 1. \end{cases} \tag{B6}$$

Then, $\chi_2^*(\xi_L)$ can be obtained by taking the Hibert transform of $\chi_1^*(\xi_L)$, i.e.

$$\chi_2^*(\xi_L) = \int_{-\infty}^{\infty}\frac{\chi_1^*(t)\,dt}{\pi(\xi_L - t)} \tag{B7}$$

which gives

$$\chi_2^*(\xi_L) = \begin{cases} -\dfrac{\mathscr{B}\left(\frac{1}{2},\frac{2-q}{2}\right)}{\pi q}F\left(1,\frac{q-1}{2};\frac{q+2}{2};\xi_L^2\right)\sin\left(\frac{q\pi}{2}\right); & |\xi_L| \le 1 \\ -\dfrac{\mathscr{B}\left(\frac{1}{2},\frac{2-q}{2}\right)}{\pi}\dfrac{1}{\xi_L^2}F\left(\frac{2-q}{2},1;\frac{1}{2};\frac{\xi_L^2-1}{\xi_L^2}\right)\sin\left(\frac{q\pi}{2}\right); & |\xi_L| \ge 1. \end{cases}$$

We can now construct the desired analytic function $\Gamma^*(\zeta_L)$ as

$$\Gamma^*(\zeta_L) = \chi(\zeta_L) - \chi^*(\zeta_L). \tag{B9}$$

Another analytic function which we need in this paper is defined as

$$\Omega^*(\bar{\zeta}_T) = -i(1-\bar{\zeta}_T^2)^{1/2}\Gamma^*(\bar{\zeta}_T). \tag{B10}$$